

Sci-Net: a Scale Invariant Model for Building Detection from Aerial Images

Hasan Nasrallah
Lebanese University
Hadath, Lebanon

Ali J. Ghandour
National Center for Remote Sensing (CNRS)
Beirut, Lebanon
aghandour@cnrs.edu.lb

Abstract—Buildings’ segmentation is a fundamental task in the field of earth observation and aerial imagery analysis. Most existing deep learning-based algorithms in the literature can be applied to fixed or narrow-ranged spatial resolution imagery. In practical scenarios, users deal with a broad spectrum of image resolution. Thus, a given aerial image often needs to be resampled to match the spatial resolution of the dataset used to train the deep learning model. However, the technique above would result in a severe degradation in the quality of the output segmentation masks. To deal with this issue, we propose in this research a Scale-invariant neural network (Sci-Net) that can segment buildings present in aerial images at different spatial resolutions. Specifically, we modified the UNet architecture and fused it with Dense Atrous Spatial Pyramid Pooling (Dense ASPP) to extract fine-grained multi-scale representations. The performance of the proposed model against several state-of-the-art models is evaluated using the Open Cities AI dataset, where Sci-Net provides a steady performance improvement margin across all resolutions available in the considered dataset.

I. INTRODUCTION

Semantic segmentation is one of the most investigated computer vision topics, where the aim is to provide a pixel-wise classification over the various desired classes in a particular image. With the current deep learning breakthrough, several fully connected neural network models are employed in semantic segmentation [18], [2], [9], [11], [14], [23], mainly for smart city applications like autonomous driving and building footprint extraction and medical applications such as tumor segmentation from CT scans.

Buildings’ footprint segmentation from aerial imagery is considered in this paper due to its significant importance in several applications such as urban planning, disaster assessment, and change analysis. State-of-the-Art (SoA) models for buildings’ segmentation can be found in the literature [5], [7], [10], [13], [15]. In addition, several online challenges have addressed deep-learning-based buildings’ segmentation topics such as different nadir-angles, non-optical and noisy data. DIUx’s xView2, SpaceNet challenges (1, 2, 4, 5 and 7), and Open Cities AI are examples of recent well-known competitions focusing on this research topic.

Existing buildings’ segmentation models are trained on a fixed spatial resolution imagery dataset. Training a robust and accurate deep learning model capable of segmenting buildings from a wide range of input spatial resolution images remains an unaddressed research problem to the best of the authors’ knowledge. State-of-the-art buildings’ segmentation models

perform well on test images of the exact spatial resolution as the training dataset used to generate the model. Test images might be of various resolutions in practical scenarios, resulting in non-optimal inference results due to two leading causes. The first issue is the fragmentation of building segments in high-resolution images. As the model fails to acquire a large enough receptive field, it becomes harder to classify pixels closer to the center of large buildings accurately. The second problem happens in low-resolution test images when the model seamlessly merges the pixels of small building instances with the background. This problem is known as under-segmentation of buildings’ instances, where the model suffers from an over-segmentation of the background, leaving false negative holes in the mask. Those two problems mentioned above are commonly addressed by resampling the test images to match the resolution of the training dataset used to generate the model. However, as the gap between inference and training image resolution increases in both directions, the quality of the resultant segmentation masks decreases.

In this context, we propose Scale-invariant neural network (Sci-Net) able to extract a multi-scale representation of an aerial image to leverage a high performance over varying spatial resolutions. The contribution of this paper is two-fold: (i) show that existing SoA buildings’ segmentation models often suffer from fragmentation, under-segmentation, or over-segmentation, (ii) introduce significant changes to the Vanilla UNet architecture encoder and decoder blocks, by integrating a Dense-ASPP module following the last block of the encoder. Sci-Net extracts better multi-scale features’ representations of the input images by employing low output stride at the decoder.

The rest of this paper is organized as follows: Section II reviews current research in the literature related to buildings’ segmentation from aerial images. Practical problems in the process of buildings’ segmentation from aerial images are discussed in Section III. Section IV introduces the proposed Sci-Net model and describes the Open Cities AI dataset, whereas Section V presents performance comparison and results. Finally, the manuscript is concluded in Section VI.

II. RELATED WORK

Existing work that focuses on capturing multi-scale context aims to capture spatial information like PSPNet [23] that integrates a Pyramid Pooling (PP) module to augment the feature

maps with pooled representation using four different bin sizes. Another methodology is implemented in DeepLabV3 [2], where the authors use dilated convolutions [22] at three different rates in their Atrous Spatial Pyramid Pooling (ASPP) module to extract multi-scale information effectively.

Authors in [13] introduce two modules: (i) channel relation module and (ii) spatial relation module modeled as composite functions. The first module applies global average pooling over the features to output channel descriptors which are later used to create a channel relation map and then multiplied with the transposed features to leverage channel augmented features. The spatial relation module comprises two 1×1 convolutions followed by matrix multiplication of the resulting weighted representations to form global spatial relation features capable of capturing global contextual dependencies for identifying various objects. Even though the authors in [13] perform their experiments on aerial scenes, the focus of their paper was to augment the extracted features with existing relations between different object instances in both the channel and spatial domain, which proved to provide a good improvement in terms of segmentation. However, the validation of their results is based on the Postdam dataset with a fixed high resolution of 5cm/pixel.

Furthermore, authors in [5] introduce the Local Feature Extractor (LFE) module composed of a series of dilated convolutions of decreasing rate after aggressively increasing the rates of dilated convolutions used in the front-end module to attain a high receptive field throughout the feature extraction process. They show that LFE module helps with tiny objects by recovering the spatial inconsistency and extracting local structure at higher layers.

In [24], authors introduce a modified version of squeeze and excitation blocks denoted as Squeeze and Attention (SA) module. SA module re-weights spatial locations in the features according to the local and global context, thus, improving semantic segmentation.

III. PROBLEM DESCRIPTION

Designing a model that is capable of segmenting building footprint included in aerial images at a different range of spatial resolution faces the following challenges:

- (i) **Features Resolution:** Most Feature extractors [17], [6], [4], [19], [16] are a series of five down-sampling stages, where each stage outputs denser and more meaningful representations than the previous one. However, features spatial resolution is reduced to half at each stage using a 2×2 pooling operation or a convolution with a stride = 2. This reduction leads to a loss in spatial information the deeper we go in the network, as the features extracted by the last stage have a resolution $32 \times$ smaller than the input size (output stride = 32).

Maintaining a sufficiently good feature resolution is crucial in segmentation, especially for tiny objects. Architectures like UNet [14] and FPN [11] make use of all extracted features from different stages to compensate for

this loss. In contrast, others try a much more computationally expensive method by maintaining a fixed high-resolution (output stride = 4) in all stages [18].

- (ii) **Field View:** in feature extraction networks, convolutions are applied with a 3×3 receptive field (kernel size). Although this works very well in segmenting small to medium-sized objects, it often fails when dealing with large objects, i.e., building footprints at very high resolutions such as 2cm/pixel. In the latter case, predicted segments often suffer from fragmentation, under-segmentation, and noise because the field of view is too small for the network to decide if the pixel belongs to a large object or the background. On the contrary, increasing receptive field by applying convolutions with an increasing kernel size leads to losing local information and exponential growth in both time and computational complexity.

The proposed Sci-Net model deals with the problems stated in point (ii) above by considering the effective use of dilated convolutions as described in the following sub-section.

A. Dilated Convolutions

Dilated convolutions work just like regular convolutions; however, they manage to increase the size of the receptive field by the insertion of holes between the weights of the kernel according to a selected rate denoted by r . For a 2-dimensional input feature map x , the output feature map y obtained as a result of a dilated convolution at every spatial location i with a rate r is defined according to the following function:

$$y[i] = \sum (x[i + r * k] * w[k]). \quad (1)$$

The rate r corresponds to the distance between the kernel weights. In this manner, a 3×3 convolution with rates = 1, 2 and 3 acquire same receptive field size as 3×3 , 5×5 , and 7×7 regular convolutions respectively with same constant number of parameters as a 3×3 regular convolution as shown in Figure 1. Using dilated convolution increases receptive field size without incurring additional time or computational complexity.

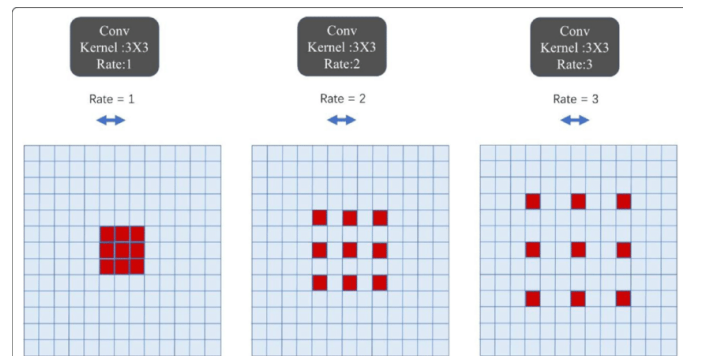


Fig. 1: Dilated 3×3 convolutions with rates = 1, 2 and 3 acquiring 3×3 , 5×5 and 7×7 receptive fields, respectively.

B. Atrous Spatial Pyramid Pooling (ASPP)

ASPP is a module that applies multiple dilated convolutions with different rates on the feature maps to capture multi-scale representations. The concept has been first introduced in [1] and then further developed in [2], [3].

Typically one 1×1 convolution, three 3×3 dilated convolutions of atrous rates equal to (8, 12 and 18), and a global average pooling layer are applied in parallel. The resulting representations are then concatenated together and pooled with a 1×1 convolution as shown in Figure 2 (a). Applying three different and separate dilated convolutions allows the model to extract spatial information at three different scales with a maximum receptive field size equal to 37 pixels.

C. Dense ASPP

Dense ASPP [21] applies dilated convolutions with increasing atrous rates in a cascade manner. The input to each dilated convolution block is the initially extracted feature maps concatenated with all the representation from previous dilated convolutions of lower rates as shown in Figure 2 (b). Typically, four atrous convolutions are applied with rates equal to (3, 6, 12 and 18). When two convolutions of different receptive fields are stacked together, the resulting receptive field increases in a linear manner, as follows:

$$R_{new} = R_1 + R_2 - 1. \quad (2)$$

where R_1 and R_2 denote receptive fields size in pixels of the 1st and 2nd convolutional layers, and R_{new} is the size of the new receptive field after stacking the two convolutional layers together.

Usage of Dense ASPP would lead to 16 receptive field scales and a maximum value equal to 79 pixels, which means that more pixels are involved in the convolution resulting in a denser feature pyramid than ASPP. Thus, based on the above analysis, Dense ASPP is integrated into the proposed Sci-Net model.

IV. FRAMEWORK

In this section, we first provide a detailed description of the proposed Sci-Net model architecture and illustrate the vital role of every change we apply to deliver a better performance. We then describe the Open Cities AI dataset used for the scope of this work. Finally, the training pipeline and environment utilized to generate performance results are presented.

A. Sci-Net Architecture

The proposed Sci-Net model shown in Figure 3 adapts conventional UNet encoder-decoder architecture [14] with the following changes to suit the purpose of this research:

- replace the encoder with a more powerful yet light-weight feature extractor from the RegNet Family; specifically, we used *RegNetY-1.6GF*. RegNets claims to perform similar to their Efficient-Net counterparts while being 3x to 5x times faster.
- integrate Dense ASPP block to extract multi-scale representation from the features of the last encoder stage.

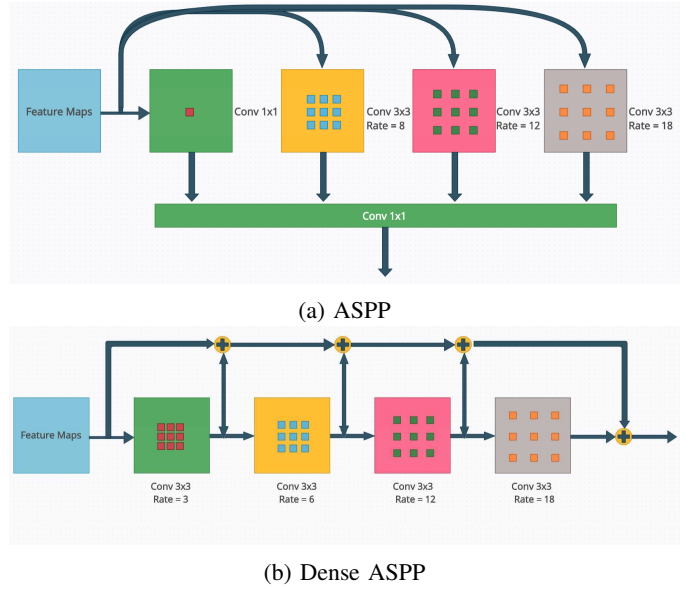


Fig. 2: ASPP vs. Dense ASPP architectures.

Dense ASPP output features are the input to the first decoder block. We used the following rates (3, 6, 12, 18) for the dilated blocks, and we set the output channels to 256 for each block. When concatenated, the multi-scale representations alone are a total of $256 \times 4 = 1024$ channels, and the initial feature maps contain 888 channels.

- substitute last 3×3 convolution of a kernel stride = 2 in the 5-th encoder stage, with a dilated convolution of a low atrous rate = 2 and kernel stride = 1 to prevent downsampling of features produced by stage 5 and thus the output stride remains equal to 16 instead of 32. This modification preserves a sufficiently good spatial resolution at the Dense ASPP input.
- Finally, no upsampling is applied at the first decoder block as both stages 4 and 5 feature maps have the exact spatial resolution.

Each decoder block comprises two 3×3 convolutions with a stride equal to 1 followed by a 2x upsampling bilinear interpolation.

B. Dataset Description

To assess the performance evaluation of the proposed Sci-Net model over different images' spatial resolution, we used the Open Cities AI Challenge dataset (also known as Segmenting buildings for disaster resilience). The majority of the data are collected across different African cities, where the images and labels quality varies from one region to another. Open Cities AI dataset is split into two tiers. For the scope of this work, tier 1 images are used, where imagery and labels are distributed under the **CC-BY-4** and **OdbL-1.0** licenses, respectively. Tier 1 data is made of 31 GeoTiff images of different spatial resolution and size. Resolution varies from very high (2cm/pixel) up to medium (20cm/pixel) resolutions.



Fig. 3: Proposed Sci-Net Architecture.

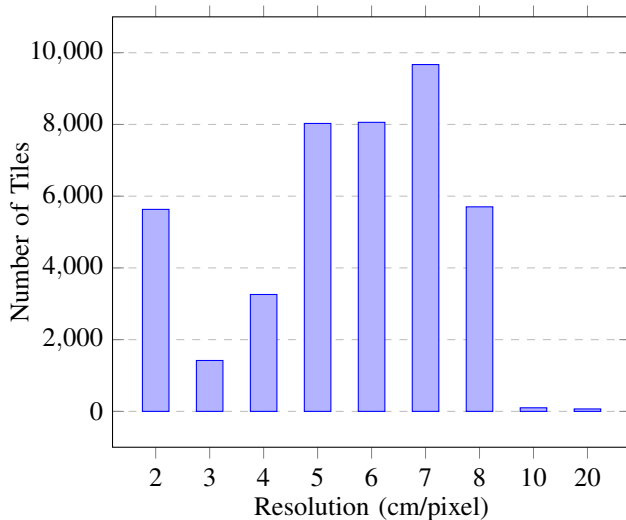


Fig. 4: Tiles distribution per resolution in cm/pixel in the Open Cities AI dataset.

Moreover, Figure 4 shows images distribution across different resolutions.

The resulting dataset contains 40,000 tiles with their corresponding buildings' masks. Finally, we used the k -folds technique to create 10 stratified folds ($k = 10$), where we balance the number of images per resolution in each fold. In our experiments, we used nine folds for training and one fold for testing with no model ensembling, as this goes beyond the scope of this paper.

C. Training Pipeline

In all our experiments, the models are trained until convergence (50 epochs) using Adam optimizer [8] and polynomial learning rate policy [23] where the learning rate is decayed from the initial one of 0.0001 till zero at the last epoch as follows:

$$lr_{t+1} = lr_t * \left(1 - \frac{epoch_{t+1}}{epoch_{max}}\right)^{0.9} \quad (3)$$

A weighted combination of Dice loss and Binary Cross-Entropy (BCE) loss is used as defined in the following:

$$\text{Loss} = \Gamma_1 \cdot BCE + \Gamma_2 \cdot Dice \quad (4)$$

where $\Gamma_1 = \Gamma_2 = 0.5$ is considered for simplicity.

During training, we use a batch-size of 12 random 512×512 chips of the original 1024×1024 tiles and apply only positional augmentations like horizontal-flipping, vertical-flipping, and 180° rotation with an 80% probability. These augmentations help in introducing some randomness at every training iteration and prevent the model from over-fitting. However, we avoided using harder augmentations like RGB-shifts, random gamma, Gaussian noise, and deformations since they would induce marginal modification to our raw data and thus require additional tuning procedures. Moreover, the training is performed over a Single Titan-XP GPU card with 12 GB of VRAM. In addition to the proposed Sci-Net model, we trained some well-known SoA models for comparison. Training these models took between 20 and 120 hours, depending on the model complexity.

Training framework is done in PyTorch using mixed precision functionalities [12] and *pytorch-segmentation-models* implementation [20].

V. EXPERIMENTAL RESULTS

A. Metrics

Performance evaluation of the proposed Sci-Net and SoA models is measured using macro, and micro Intersection over Union (IoU) and F1-score defined below:

$$IoU = \frac{TP + \varepsilon}{TP + FP + FN + \varepsilon} \quad (5)$$

$$F1 - score = \frac{(1 + \beta^2) \cdot TP + \varepsilon}{(1 + \beta^2) \cdot TP + \beta^2 \cdot FN + FP + \varepsilon} \quad (6)$$

where $\beta = 1$ and $\varepsilon = 0.0001$. TP , FP , and FN are True Positive, False Positive, and False Negative, respectively.

The employed metrics are used according to the following two types of averaging across the whole test dataset:

- 1) **Macro** scores are calculated per prediction according to TP , FP , and FN for each prediction mask and then averaged afterward.
- 2) **Micro** scores are calculated using the total number of TP , FP , and FN across all prediction masks, and then the final score is computed accordingly.

Macro scoring helps in assessing the average performance per image, while micro scoring assesses the overall performance. Correctly classified images with blank ground truth masks (True Negative) provide a boost in macro scoring. However, such images do not affect micro scoring, as it treats the whole dataset as having one large ground truth mask.

It is worth noting that simulation results are validated every epoch, and the model’s weights that maximize micro-IoU score over the validation set are saved.

B. Performance

Experimental results reveal the performance superiority of the proposed Sci-Net over several SoA models in terms of IoU and F1-score across varying resolutions. At inference time, the images are fed to the neural network at full scale (1024×1024). Table I shows that the proposed Sci-Net model provides at least 2% score improvement over benchmarked SoA models. Sci-Net attained a micro-IoU score of 82.25% on the test set, which is better by a margin than its nearest competitor (UNet+ASPP) with a relative score of 80.47%. Table I also shows that Sci-Net scored the highest macro-IoU value of 88.42%, which indicates that it leverages the best per-image performance. Furthermore, the 2% minimum score improvement margin is observed in micro and macro F1-scores (91.04% and 92.62% respectively). Thus, the proposed model attains better precision and recall against competitor models. Models like PSPNet and DeepLabV3+ failed to provide near good results at some resolutions leading to a degradation in their scores.

Furthermore, we plot micro and macro IoU and F1-scores for each resolution (cm/pixel) for every model as shown in Figure 5. The green curve corresponding to the Sci-Net model always performs better than all other models across different metrics, which shows that it can effectively extract

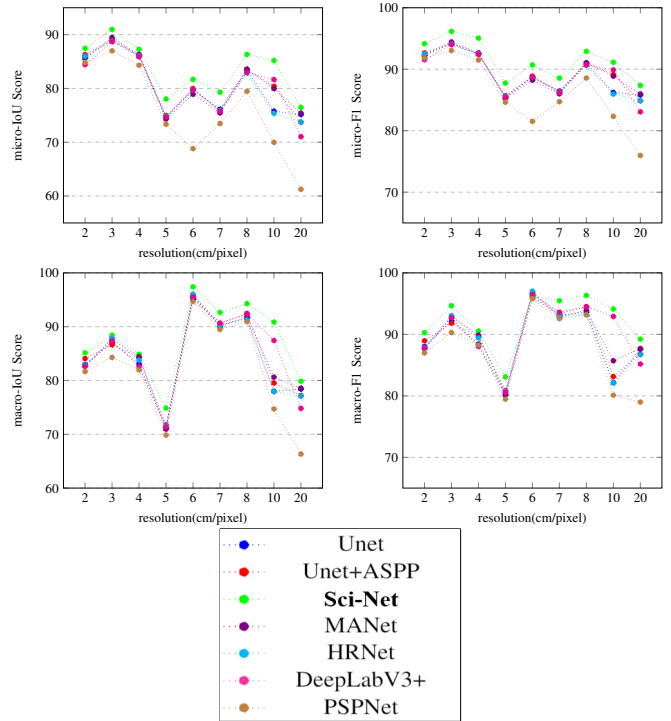


Fig. 5: Performance comparison of Sci-Net (in green) versus SoA models in terms of micro- and macro- IoU and F1 scores.

better multi-scale representations than any existing models. Sci-Net curve is consistently above all other curves for the four presented score graphs, which indicates that it is less prone to performance degradation when the scale changes. It is unclear which model holds the “runner up” spot, as these models alternate places on varying resolutions. For instance, UNet+ASPP (in red) achieves competitive scores for resolutions in range (2cm/pixel up-to 8cm/pixel), however its performance deteriorates for larger resolutions. PSPNet (in brown) benchmarks the worst performance for all resolutions.

To better visualize our results, sample predicted masks by each model are shown in Figure 6. For instance, problems like fragmentation and under-fitting are solved using Sci-Net by acquiring sufficiently large receptive fields capable of relating far pixels that belong to large building instances at high resolutions (Masks in rows 1, 2, 3, and 4). In the first four rows, it is clear that Sci-Net succeeds in segmenting large building instances. For example, models like DeepLabV3+, UNet, and HRNet showed a critical level of mask fragmentation for that large building instance in the first row. Also, at lower resolutions (rows 6 and 7), Sci-Net can avoid over-segmentation, unlike other architectures such as HRNet that misclassified a significant amount of background pixels, as shown in row 6.

While models that use pyramid pooling like PSPNet performed well in segmenting large building instances (row 1 and 2), they often failed in capturing all small to medium-sized buildings at lower resolutions. Finally, Unet+ASPP could

Model	micro-IoU	micro-F1	macro-IoU	macro-F1
PSPNet	78.47	87.93	85.04	89.55
DeepLabV3+	79.83	88.78	86.28	90.50
MANet	80.08	88.93	86.20	90.38
UNet	80.18	89.00	86.01	90.16
HRNet	80.30	89.07	82.85	90.46
UNet+ASPP	80.47	89.18	86.65	90.79
Sci-Net	82.25	91.04	88.42	92.62

TABLE I: Performance metrics of Sci-Net architecture compared to existing SoA models on the testset.

not capture enough multi-scale information to segment large structures properly (rows 1, 2, and 3). Sci-Net proved to be the most efficient at all the presented resolutions, as shown in Figure 6.

VI. CONCLUSION

This paper proposes Sci-Net, a new model capable of accurately segmenting buildings’ footprint at multi-scale spatial resolutions. We compare the performance of Sci-Net with other well-known SoA models. We show that the proposed Sci-Net architecture does not suffer from fragmentation, over-segmentation, and under-segmentation problems.

REFERENCES

- [1] Liang-Chieh Chen, George Papandreou, Iasonas Kokkinos, Kevin Murphy, and Alan L. Yuille. Deeplab: Semantic image segmentation with deep convolutional nets, atrous convolution, and fully connected crfs. *CoRR*, abs/1606.00915, 2016.
- [2] Liang-Chieh Chen, George Papandreou, Florian Schroff, and Hartwig Adam. Rethinking atrous convolution for semantic image segmentation. *CoRR*, abs/1706.05587, 2017.
- [3] Liang-Chieh Chen, Yukun Zhu, George Papandreou, Florian Schroff, and Hartwig Adam. Encoder-decoder with atrous separable convolution for semantic image segmentation. *CoRR*, abs/1802.02611, 2018.
- [4] Yunpeng Chen, Jianan Li, Huaxin Xiao, Xiaojie Jin, Shuicheng Yan, and Jiashi Feng. Dual path networks. *CoRR*, abs/1707.01629, 2017.
- [5] Ryuhei Hamaguchi, Aito Fujita, Keisuke Nemoto, Tomoyuki Imaizumi, and Shuhei Hikosaka. Effective use of dilated convolutions for segmenting small object instances in remote sensing imagery. *CoRR*, abs/1709.00179, 2017.
- [6] Kaiming He, Xiangyu Zhang, Shaoqing Ren, and Jian Sun. Deep residual learning for image recognition. *CoRR*, abs/1512.03385, 2015.
- [7] Vladimir I. Iglovikov, Selim S. Seferbekov, Alexander V. Buslaev, and Alexey Shvets. Ternausnetv2: Fully convolutional network for instance segmentation. *CoRR*, abs/1806.00844, 2018.
- [8] Diederik P Kingma and J Adam Ba. A method for stochastic optimization. arxiv 2014. *arXiv preprint arXiv:1412.6980*, 434, 2019.
- [9] Hanchao Li, Pengfei Xiong, Jie An, and Lingxue Wang. Pyramid attention network for semantic segmentation. *CoRR*, abs/1805.10180, 2018.
- [10] Qingyu Li, Yilei Shi, Stefan Auer, Robert Roschlaub, Karin Möst, Michael Schmitt, Clemens Glock, and Xiaoxiang Zhu. Detection of undocumented building constructions from official geodata using a convolutional neural network. *Remote Sensing*, 12(21), 2020.
- [11] Tsung-Yi Lin, Piotr Dollár, Ross B. Girshick, Kaiming He, Bharath Hariharan, and Serge J. Belongie. Feature pyramid networks for object detection. *CoRR*, abs/1612.03144, 2016.
- [12] Paulius Micikevicius, Sharan Narang, Jonah Alben, Gregory F. Diamos, Erich Elsen, David Garcia, Boris Ginsburg, Michael Houston, Oleksii Kuchaiev, Ganesh Venkatesh, and Hao Wu. Mixed precision training. *CoRR*, abs/1710.03740, 2017.
- [13] Lichao Mou, Yuansheng Hua, and Xiao Xiang Zhu. A relation-augmented fully convolutional network for semantic segmentation in aerial scenes. *CoRR*, abs/1904.05730, 2019.
- [14] Olaf Ronneberger, Philipp Fischer, and Thomas Brox. U-net: Convolutional networks for biomedical image segmentation. *CoRR*, abs/1505.04597, 2015.
- [15] Yilei Shi, Qingyu Li, and Xiao Xiang Zhu. Building segmentation through a gated graph convolutional neural network with deep structured feature embedding. *CoRR*, abs/1911.03165, 2019.
- [16] Christian Szegedy, Sergey Ioffe, and Vincent Vanhoucke. Inception-v4, inception-resnet and the impact of residual connections on learning. *CoRR*, abs/1602.07261, 2016.
- [17] Mingxing Tan and Quoc V. Le. Efficientnet: Rethinking model scaling for convolutional neural networks. *CoRR*, abs/1905.11946, 2019.
- [18] Jingdong Wang, Ke Sun, Tianheng Cheng, Borui Jiang, Chaorui Deng, Yang Zhao, Dong Liu, Yadong Mu, Mingkui Tan, Xinggang Wang, Wenyu Liu, and Bin Xiao. Deep high-resolution representation learning for visual recognition. *CoRR*, abs/1908.07919, 2019.
- [19] Saining Xie, Ross B. Girshick, Piotr Dollár, Zhuowen Tu, and Kaiming He. Aggregated residual transformations for deep neural networks. *CoRR*, abs/1611.05431, 2016.
- [20] Pavel Yakubovskiy. Segmentation models pytorch, 2020.
- [21] Maoke Yang, Kun Yu, Chi Zhang, Zhiwei Li, and Kuiyuan Yang. Denseaspp for semantic segmentation in street scenes. In *Proceedings of the IEEE Conference on Computer Vision and Pattern Recognition (CVPR)*, June 2018.
- [22] F. Yu and V. Koltun. Multi-scale context aggregation by dilated convolutions. *CoRR*, abs/1511.07122, 2016.
- [23] Hengshuang Zhao, Jianping Shi, Xiaojuan Qi, Xiaogang Wang, and Jiaya Jia. Pyramid scene parsing network. *CoRR*, abs/1612.01105, 2016.
- [24] Zilong Zhong, Zhong Qiu Lin, Rene Bidart, Xiaodan Hu, Ibrahim Ben Daya, Jonathan Li, and Alexander Wong. Squeeze-and-attention networks for semantic segmentation. *CoRR*, abs/1909.03402, 2019.

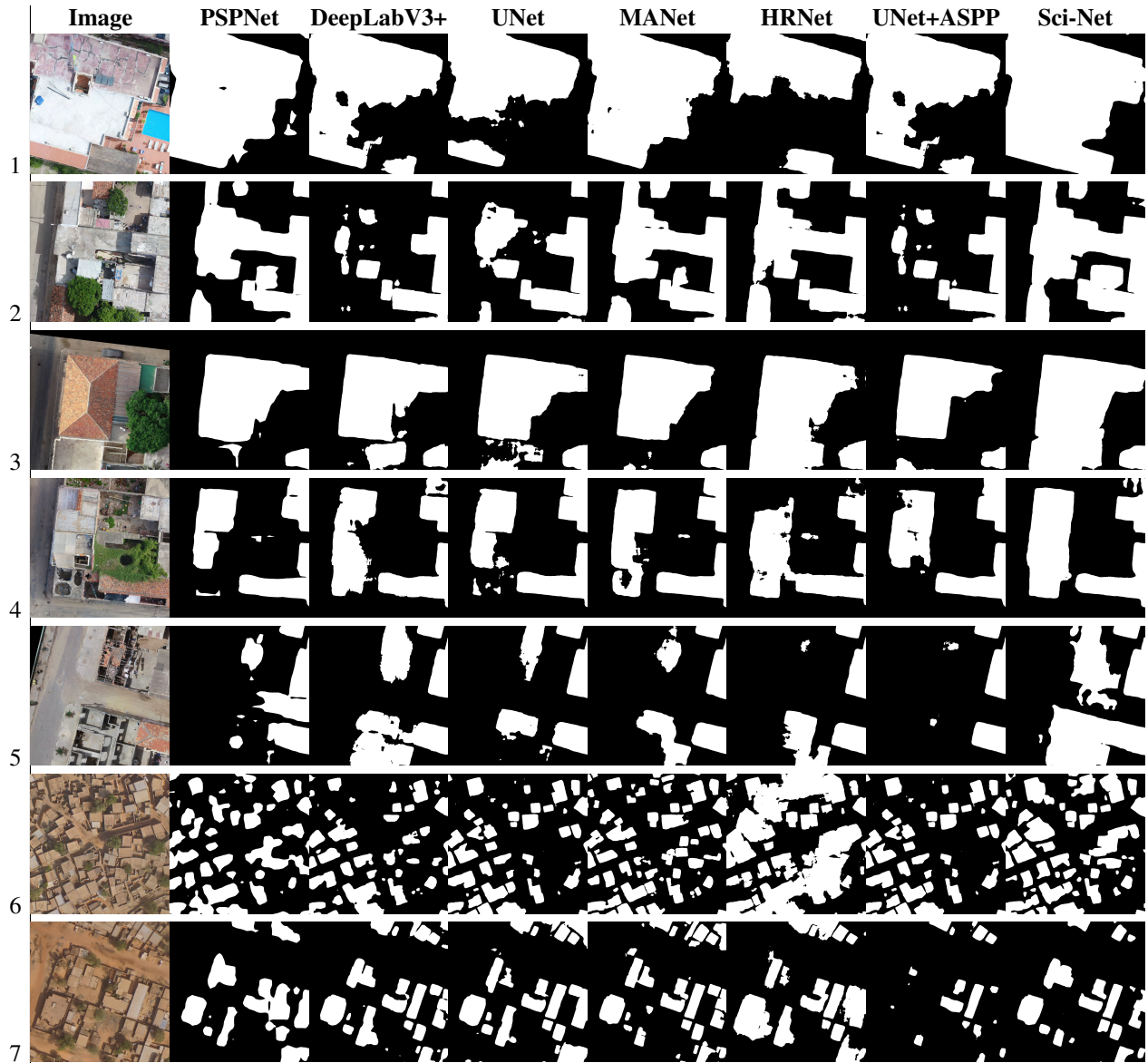


Fig. 6: Predicted masks for Sci-Net and benchmarked SoA models for various images at different resolutions revealing fragmentation, under- and over-segmentation issues.